



Effect of absorption enthalpy on temperature-swing CO₂ separation process performance

Citation

Van Nierop, Ernst A., Sahand Hormoz, Kurt Z. House, and Michael J. Aziz. 2011. "Effect of Absorption Enthalpy on Temperature-Swing CO₂ Separation Process Performance." *Energy Procedia* 4: 1783–1790. doi:10.1016/j.egypro.2011.02.054.

Published Version

doi:10.1016/j.egypro.2011.02.054

Permanent link

<http://nrs.harvard.edu/urn-3:HUL.InstRepos:34264570>

Terms of Use

This article was downloaded from Harvard University's DASH repository, and is made available under the terms and conditions applicable to Other Posted Material, as set forth at <http://nrs.harvard.edu/urn-3:HUL.InstRepos:dash.current.terms-of-use#LAA>

Share Your Story

The Harvard community has made this article openly available.
Please share how this access benefits you. [Submit a story](#).

[Accessibility](#)



GHGT-9

Effect of absorption enthalpy on temperature-swing CO₂ separation process performance

Ernst A. van Nierop^{a*}, Sahand Hormoz^b, Kurt Z. House^a, Michael J. Aziz^b

^a*C12 Energy, 24 Thorndike St., Cambridge MA 02141, USA*

^b*School of Engineering and Applied Sciences, Harvard University, Cambridge MA 02138, USA*

Abstract

We model a CO₂ absorption process to elucidate the rationale for the search for a solvent with an enthalpy of absorption (ΔH) of low magnitude. We explore the relationship between ΔH and the system's performance. While in general a lower magnitude appears to provide better system performance because it permits the stripper temperature to be decreased, as the magnitude drops below its value for monoethanolamine amine (MEA), 80 kJ/mol, the required solvent mass flow rate must increase precipitously and/or the flue gas must be cooled significantly. We argue that the associated parasitic pumping and cooling loads, as well as the increased capital cost, may set a practical lower limit on the magnitude of the enthalpy of absorption that is not very different from that of MEA.

© 2011 Published by Elsevier Ltd.

Keywords: TSA systems; CO₂ capture process performance; enthalpy of absorption; MEA.

1. Introduction

As power plant scale CO₂ post-combustion capture systems around the world move from pilot project to full scale commercial deployment, many of the classical solvent (or sorbent) absorber/stripper systems currently on the market are likely to be deployed. In such temperature or pressure swing absorber (TSA or PSA) systems, the final process design presumably optimizes levelized costs based on solvent/sorbent properties and a host of more site-specific variables. Here, we restrict our analysis to TSA systems with solvents, but the spirit of the discussion also applies to PSA systems with sorbents.

The role of the solvent is key, and a good solvent is generally characterized by the following properties [1, 2]: (i) high selectivity for CO₂, (ii) low propensity to degrade over time, (iii) high maximum solvent loading, (iv) low lifetime cost, (v) wide envelope of possible operating conditions (pressure, temperature), and finally, (v) low enthalpy of absorption (ΔH). The importance of this final property is often directly linked to the energy penalty that the CO₂ scrubber system imposes on the power plant. On the one hand, a 'large' ΔH (i.e. large magnitude) is indicative of a solvent with a high affinity for CO₂, but on the other hand, for any amount of heat that is released in

* Corresponding author. Tel.: +1-617-849-8006.

E-mail address: ernst@c12energy.com

the absorber, an even larger quantity of heat must be supplied to the stripper. As a consequence, much research is devoted to the search for a solvent with a ‘small’ ΔH (i.e. small magnitude), see for example [2–4].

The heat provided to the stripper is often broken into three separate pieces: (1) sensible heat to bring the stream of rich amine up to the operating temperature of the stripper; (2) enthalpy of reaction to reverse the CO_2 absorption; and (3) heat to vaporize water in the stripper to drive the desorption reaction forward by removing CO_2 as it is released out of the stripper. How much sensible heat and ‘stripping’ heat is required depends rather indirectly on ΔH ; furthermore the heat supplied to the stripper does not make up the entire energy penalty of the CO_2 scrubber system. Direct cooling loads, and the electric energy required to compress the CO_2 after separation are also main contributors. Clearly, system performance depends on more factors than just ΔH , and in some cases a large ΔH proves to be the more favorable choice [5, 6]. In this work we aim to gain a better understanding of the relevant importance of ΔH , by modeling a generic TSA system and keeping all solvent properties constant except ΔH .

2. Thermodynamic Background

As discussed in [7], in the most thermodynamically abstract sense, a temperature-swing CO_2 absorption & separation process (TSA) can be depicted as an engine that takes heat from a hot reservoir (T_H), and uses this heat (Q) to internally do work (W) on a stream of flue gas (see figure 1). In separating the flue gas into its main components, nitrogen and carbon dioxide, the heat engine rejects heat to a cold reservoir (the environment, at temperature $T_e = T_L$). In this most abstract formulation, it is clear that the maximum efficiency of the internal heat-to-work engine is limited by the Carnot efficiency, $W/Q_{\text{net}} = \eta_C = 1 - T_L/T_H$, and the hot reservoir’s temperature corresponds to the temperature of the stripper. The minimum work required to separate a fraction f of CO_2 from a gaseous stream with CO_2 mol fraction x is ([7])

$$W_{\min} = RT \frac{1}{x} \left[(1-f)x \ln \left(\frac{(1-f)x}{1-fx} \right) + (1-x) \ln \left(\frac{(1-x)}{1-fx} \right) - x \ln(x) - (1-x) \ln(1-x) \right], \quad (1)$$

where R is the universal gas constant, and T is temperature. For typical conditions of $x = 0.12$ and $f = 0.9$, $W_{\min} \approx 8$ kJ/mol. Given that the heat that is provided to run this CO_2 -separation machine is typically taken from the steam cycle of a power plant where it would have been used to generate power, it is appropriate to consider the loss of *exergy* or availability associated with the CO_2 scrubber [8]. A natural figure of merit for a CO_2 separation system is thus the exergy loss per mol of CO_2 captured and compressed. By looking at exergy (i.e. $Q_{\text{heat}} \eta_C$) rather than just Q_{heat} , we place an appropriate premium on high temperature heat.

For a given CO_2 exit partial pressure, the performance of the CO_2 scrubber varies with ΔH . This is demonstrated in figure 2 where we have plotted the equilibrium vapor pressure of CO_2 over a solution of CO_2 solvent for different temperatures (see (3)). The curve corresponding to $\Delta H = -80$ kJ/mol corresponds to equilibrium data for mo-

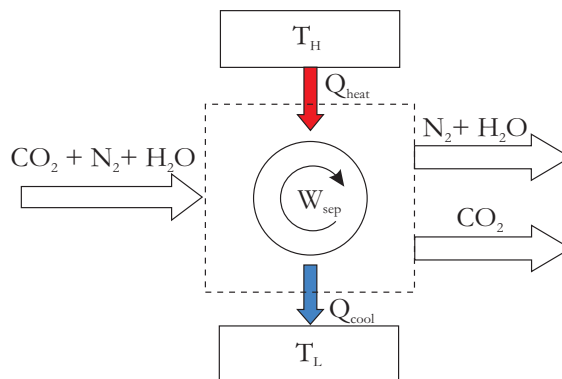


FIG. 1. Abstracted representation of a thermal CO_2 separation engine.

noethanolamine (MEA) from [9, 10], while the other curves use some data for MEA (i.e. the entropy of the overall reaction, and the concentration & loading dependence) but alter ΔH (see Table 1 in [9]). Note that the y-axis cutoff for the logarithm of the partial pressure (p_{CO_2}) is directly related to $\Delta S^{0*}/R$, where ΔS^{0*} is the entropy of the overall dissolution / absorption reaction at standard conditions. This is important to note since most solvents have very similar ΔS^{0*} (for the family of the alkanolamines, for example, the spread is less than 9% [9]). This entropy change is dominated by the entropy loss of the CO_2 molecule upon going from an ideal gas state to a liquid state relatively low entropy, and cannot be expected to vary greatly from one liquid to another. Thus we set the point on the y-axis from which all other curves, regardless of ΔH , emanate. If one chooses the operating partial pressures of CO_2 in a TSA absorber and stripper respectively; a particular ΔH will set the required operating temperatures as shown in figure 2. The associated Carnot efficiency *increases* with increasing $|\Delta H|$, since the ‘hot’ temperature T_H increases accordingly, but the cooler environment temperature (T_c) to which heat will eventually be rejected stays the same.

From observation of figure 2 we can understand why the chilled ammonia process (with $\Delta H \approx -60$ kJ/mol, [11]) necessarily runs at an absorber temperature close to 273 K, but we also see that this means that it will have a relatively low internal Carnot efficiency. Of course, this ‘first-order’ view of the process neglects the fact that solvent loading can impact the p_{CO_2} vs. ΔH curve, as well as other process considerations. However, the role of ΔH in setting overall process performance is not obvious.

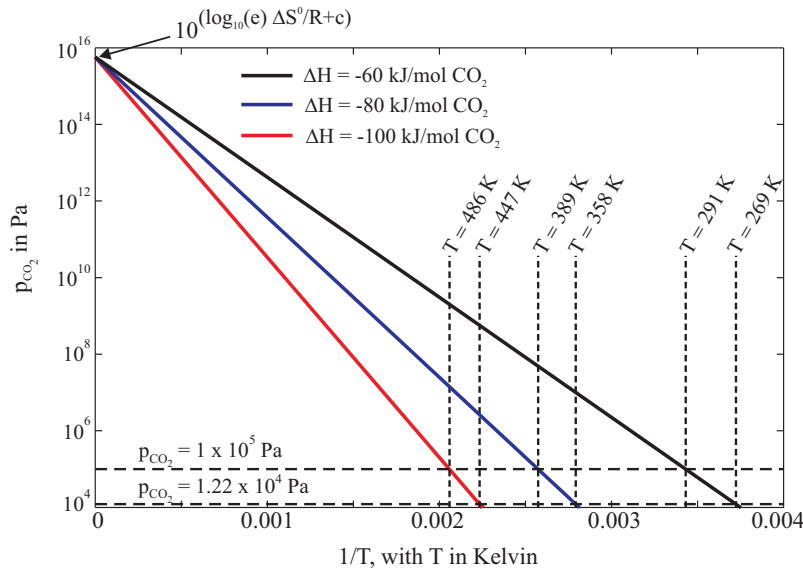


FIG. 2. Partial pressure of CO_2 over an amine solution with different ΔH . The required temperatures in the absorber and stripper are set by ΔH and the required operating pressures (which are assumed to be equal to the equilibrium p_{CO_2}).

3. Model Development

3.1. Process chemistry

Our model is a straightforward mass- and heat balance based on equilibrium thermodynamics, and implemented in MATLAB. It operates with a solvent that is ‘MEA-like’, meaning that the CO_2 absorption reaction chemistry (and related mass balance) is akin to that of CO_2 and MEA, i.e.,



where MEA is a place holder for any other similar solvent. In the case of MEA, MEAC is more accurately the

carbamate associated with MEA (i.e. $\text{HO}(\text{CH}_2)_2\text{NHCOO}^-$) while MEAH is the protonated solvent molecule (i.e. $\text{NH}_2(\text{CH}_2)_2\text{OH}_2^+$). This process chemistry was chosen since there is a lot of data available for MEA; but the model is easily altered for any other reaction stoichiometry.

3.2. Process description

Actual TSA processes are decidedly more complex than the abstract depiction presented in figure 1, but they are certainly subject to the same fundamental thermodynamic limits. In order to extend the abstract analysis of the system in figure 1 to include ΔH , we zoom in on the dotted box to separate out the typical subsystems separately; as in figure 3.

Warm moist flue gas exiting a wet flue gas desulfurization (FGD) unit at $T_0 = 328\text{K}$ [12] is first cooled down to T_1 in the pre-conditioning unit which removes heat (Q_{PC}) by heat exchange with the cooler environment (i.e. cooling water at $T_e = T_L$). In the case where $T_1 < T_e$, further refrigeration work is required (W_{ref}), and such a refrigerator is assumed to have a $\text{COP} = T_1/(T_e - T_1)$, powered by a heat engine that runs between the hot (T_H) and cold (T_L) sinks. The pre-conditioned flue gas then enters the adiabatic absorber.

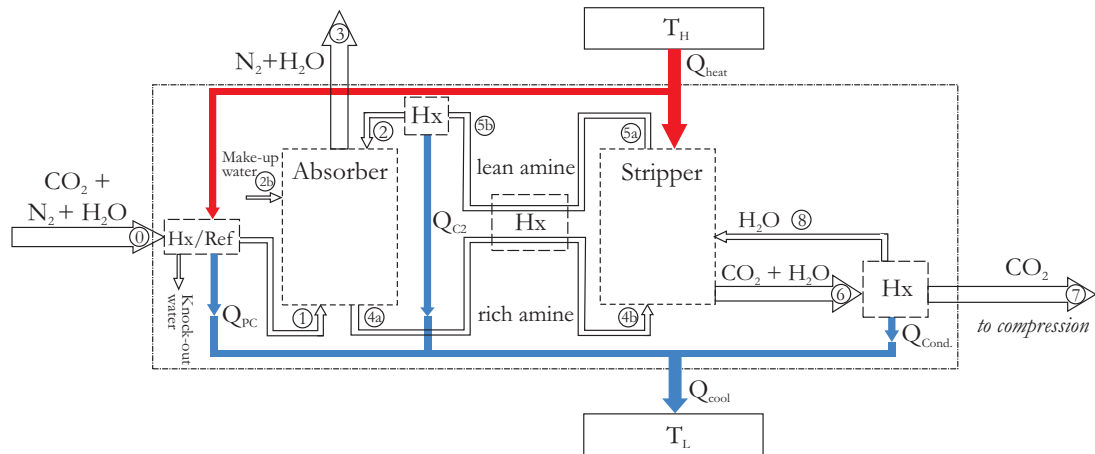


FIG. 3. System under scrutiny in this paper. Note that the pre-conditioning system (labeled “Hx/Ref”) can include refrigeration to allow $T_1 < T_L$.

In the absorber, CO_2 -rich flue is contacted with lean amine ($\theta = 0.05$) and the exiting streams of CO_2 -lean flue and CO_2 -rich amine are assumed to be at equal temperatures ($T_3 = T_{4a}$), as set by the release of ΔH in the absorber. We also specify the pressure in the absorber (p_3) to be just over 1 bar, and perform all calculations for a flow of 1 mol of CO_2 per second entering in stream 1, while assuming a 90% capture fraction. We assume that the partial pressure of CO_2 in the flue gas entering the absorber is equal to the equilibrium saturation partial pressure of CO_2 associated with the exiting rich amine stream (i.e. streams 1 and 4). In particular, we use the empirical equilibrium correlation between CO_2 partial pressure and solvent temperature, concentration, and loading as documented by Gabrielsen et. al. [9]

$$p_{\text{CO}_2} = \exp\left(A + \frac{(-\Delta H)}{RT} + Ca_0\theta\right) \frac{\theta^2}{(1 - 2\theta)^2} \quad (\text{in kPa}), \quad (3)$$

where $A \propto \Delta S^0/R$, a measure of the overall change of entropy associated with the process of dissolution and absorption; $C = -7187$, a_0 is the initial concentration of amine (mol MEA/mol solvent, roughly 0.1123 for an MEA solution

of 30% by weight as used in this work) and θ is the solvent loading (mol CO₂/mol MEA, for MEA $\theta_{max} = 0.5$).

We further take the water vapor partial pressure to be $p_{3,H_2O} = x_{4,H_2O} p_{H_2O,sat}(T_3)$, where $x_{i,j}$ denotes the mol fraction of component j in stream i , and $p_{H_2O,sat}(T)$ is the water saturation pressure at temperature T given by the Antoine equation. Consequently, since $T_3 > T_1$, some water is ‘lost’ in the absorber, and this is replenished by make-up water entering at temperature T_e in stream 2b. Using (3) together with a heat and mass balance that accounts for water loss, the model calculates the required solvent flowrate, loading, and the temperature in the absorber.

From the absorber, the CO₂-rich amine goes through an ideal heat exchanger (i.e. no heat lost to the environment) where its temperature is raised to T_{4b} by the hot lean amine exiting the stripper (using heat capacity data from [13]). The warm rich amine then enters the stripper where the CO₂ is stripped out of solution. We specify the temperature in the stripper (i.e. $T_5 = T_{5a} = T_6$), and provide enough Q_{heat} to reach the required temperature, reverse the absorption reaction, and provide stripping steam. The model calculates the stripper pressure, and the mass ratio of CO₂ to H₂O in stream 6, as well as Q_{heat} . In order to do this, we again assume that the partial pressure of CO₂ in stream 6 is equal to the saturation partial pressure of CO₂ in the rich incoming amine (stream 4) at temperature T_{4b} .

The CO₂ + H₂O stream exiting the stripper is cooled to T_e (cooling load Q_{cond}); and the condensed water is returned at temperature T_e to the stripper. The CO₂ then exits the scrubber system, and is compressed isothermally to $p_F = 100$ bar (i.e. $W_{comp} = n_{7,CO_2} R T \ln(p_F/p_7)$, which assumes CO₂ to act as an ideal gas [4]). For the final figure of merit of the overall system, we include this compression work. Simultaneously, the lean (but warm) amine is cooled (Q_{C2}) from T_{5b} to reach T_2 , closing the solvent cycle.

4. Results and Discussion

4.1. Model performance

Figures 4 and 5 indicate typical model outputs showing (i) solvent flowrate, (ii) solvent loading, (iii) stripper pressure, and (iv) CO₂/H₂O mass ratio in stream 6 respectively; as a function of the enthalpy of reaction (ΔH) and the prescribed stripper temperature. As the magnitude of the absorption enthalpy drops from 90 to 60 kJ/mol, CO₂ loading in the rich solvent drops precipitously. In order to take up enough CO₂ to achieve 90% capture, the solvent flow rate must rise precipitously. This result can be understood using figure 2. To attain the maximum possible CO₂ loading of the rich amine exiting the absorber, its saturation CO₂ pressure must be no greater than 12.2 kPa (the lower horizontal dashed line). This requirement sets a maximum permissible exit temperature that depends on the value of ΔH and is indicated as the intersection of the various curves with this dashed line. When the magnitude of ΔH drops enough that this temperature drops below the inlet flue stream temperature T_1 , the rich amine exit stream cannot leave maximally loaded. So as the magnitude of the absorption enthalpy drops significantly below the value of 80 kJ/mol characteristic of MEA, the requisite pumping hardware and its parasitic load must be increased substantially. Although we do not include these costs in this model, we point out that this criterion may determine a practical lower limit on the

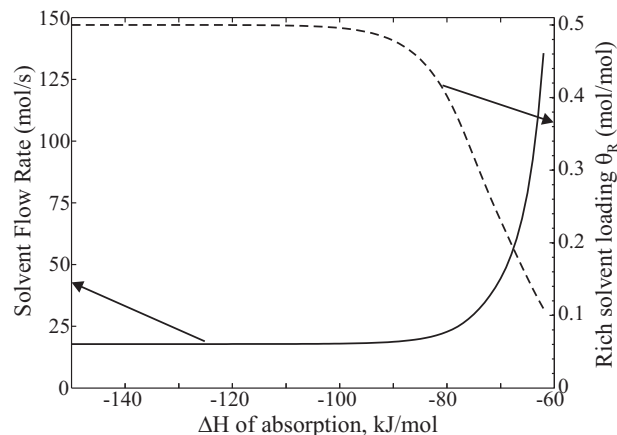


FIG. 4. Flowrate of solvent and resultant solvent loading (rich phase) ($T_1 = 313$ K).

magnitude of the absorption enthalpy near that of MEA.

Figure 5A shows the pressure in the stripper (p_6) that would result from a given choice of ΔH and $T_s = T_6$. The figure shows that stripper pressure depends mainly on temperature, and the pressure becomes excessive as $T_s \geq 400$ K. Actual systems are expected to operate in this temperature range. Figure 5B shows the $\text{CO}_2/\text{H}_2\text{O}$ mass ratio that is to be expected at a given (T_s , ΔH) combination. Again, for typical operating conditions (i.e. $\Delta H_{\text{MEA}} = -82$ kJ/mol CO_2 [9]) our model tends to overestimate this $\text{CO}_2/\text{H}_2\text{O}$ ratio. From figures 5A and 5B, we learn that our model's dependence on equilibrium data may not yield quantitatively accurate results for these elevated temperatures and dynamic conditions. However, we expect qualitative trends to persist.

Note that the white areas in figures 5 and 6 correspond to unphysical combinations of T_s and ΔH . In each of these figures, the white patch in the lower left hand corner represents a zone where T_s is too low to accommodate the relatively large magnitude of ΔH . As T_1 is decreased, so is the required minimum stripper temperature; this is related to the lower flowrate (and consequently higher solvent loading) that comes with a decrease in T_1 . The white patch on the right of each figure (independent of T_s) stems directly from the maximum accessible CO_2 partial pressure in the absorber at a given ΔH and T_1 , as depicted in figure 2. Further shifts in the regions of 'unphysical' solutions can be accomplished by altering the ΔS^{0*} of the overall reaction, and/or the concentration dependence in (3).

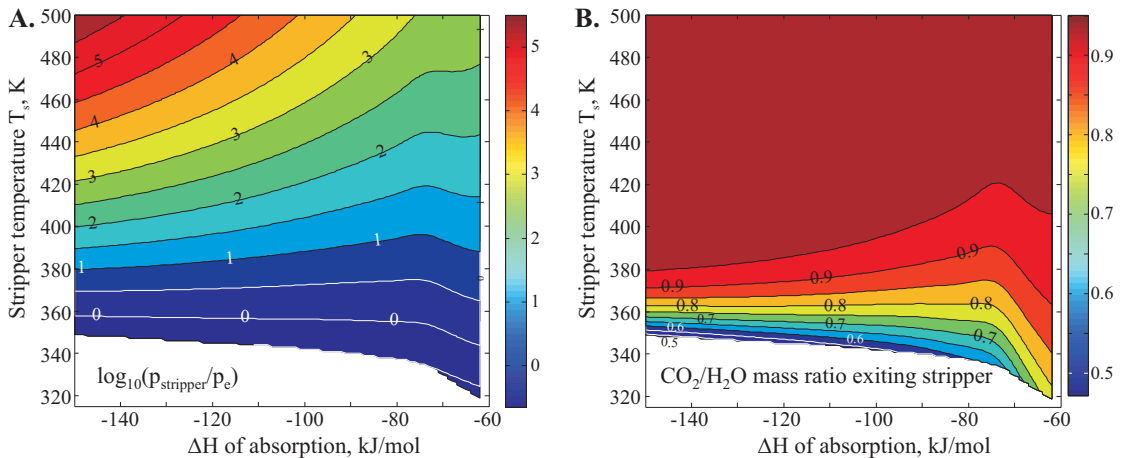


FIG. 5. (A) Pressure in the stripper on a logarithmic scale; the contour "0" corresponds to $p_s = 1$ atm., "1" corresponds to 10 atm., and so on. (B) Mass ratio of CO_2 to H_2O exiting the stripper.

4.2. System performance as a function of ΔH

As discussed, we define a figure of merit (FOM) for the CO_2 capture system by considering the total exergy (or availability) that is 'consumed' in the separation and compression of CO_2 , per mol of CO_2 . Specifically, we calculate

$$\text{FOM} = (Q_{\text{heat}}\eta_C(T_s) + W_{\text{comp}} + W_{\text{ref}}) / n_7, \quad (4)$$

where W_{ref} is the work required to refrigerate the flue gas when $T_1 < T_e$, and $\eta_C(T_s) = 1 - T_e/T_s$ while n_7 is the number of moles of CO_2 that are captured and compressed by the quantities of work and heat presented here. Clearly, a complete exergy analysis would include more contributions such as the kinetic energy in the various flows under consideration, along with additional losses that occur in the system such as frictional losses and pump- and heat exchanger efficiencies, etc. However, the figure of merit in (4) provides, in a thermodynamic sense, the most 'fair' measure of system performance, since the loss of availability represents the useful work that could have been obtained from the heat if it had not been applied to CO_2 separation.

Armed with the figure of merit as defined in (4), we interrogate our model to learn about system performance as a function of T_s , ΔH , and T_1 . Figure 6 shows that system performance is a rather complex function of ΔH , even in the absence of further complicating factors such as solvent degradation issues etc. In general, system performance

improves with decreasing ΔH , but for any given T_s local minima exist, see for instance figure 6B at $T_s = 380\text{K}$ for ΔH between -75 and -90 kJ/mol CO_2 . The complex nature of the ‘ ΔH , FOM’-landscape is the result of different non-linear contributions to the figure of merit (4). Notably, as stripper pressure increases, the amount of work required for subsequent compression decreases. When designing actual systems, however, solvent degradation at high pressure, and the capital cost associated with high operating pressures, may prove to be excessive.

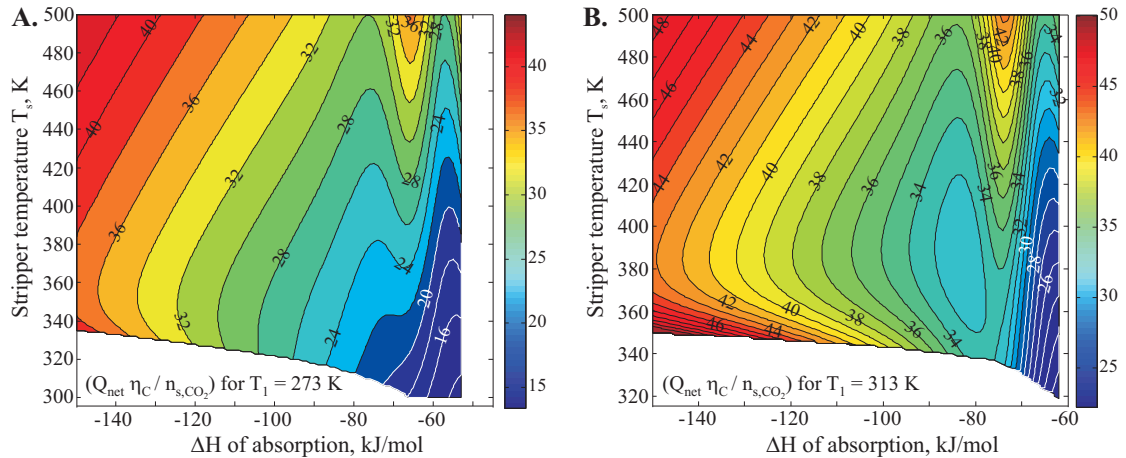


FIG. 6. (A) $T_1 = 273$ K, (B) $T_1 = 313$ K. The figure of merit depicted here is described in the text and includes compression.

Comparing figures 6A and 6B, we see the significant effect that T_1 has on system performance. Across the board, a lower T_1 seems to result in better system performance, but note that chilled systems have a greater cooling load, as shown in figure 7. Some of the heat carried away by the cooling streams indicated in figure 3 may have further beneficial use, but most of the heat is going to be very low grade and will thus directly impact cooling water pumping requirements at the power plant.

In summary, we have modeled a typical TSA CO_2 scrubbing system using an equilibrium thermodynamic approach. Subsequent interrogation of the model with respect to the role of the enthalpy of absorption reveals the relationship between ΔH and the system’s performance. While in general a lower magnitude of the absorption en-

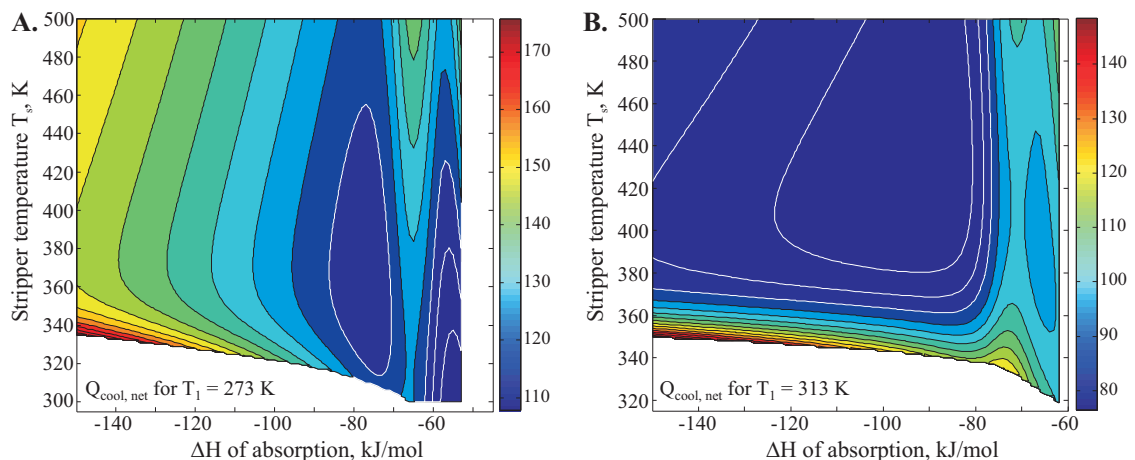


FIG. 7. (A) $T_1 = 273$ K, (B) $T_1 = 313$ K. Cooling load, combining pre-conditioning, amine cooling, and water condensation.

thalpy appears to provide better system performance because it permits the stripper temperature to be decreased, as the magnitude of ΔH drops below its value for MEA, 80 kJ/mol, the required solvent mass flow rate must increase precipitously and/or the flue gas entering the system must be chilled significantly. The associated parasitic pumping and cooling loads, as well as the increased capital cost, while not included in the present model, may set a practical lower limit on the magnitude of the enthalpy of absorption that is not very different from that of MEA.

-
- [1] Aronu U. E., Svendsen H. F., Hoff K. A., Juliussen O.. Solvent selection for carbon dioxide absorption *Energy Procedia*. 2009;1:1051-1057.
 - [2] Goto K., Okabe H., Shimizu S., Onoda M., Fujioka Y.. Evaluation method of novel absorbents for CO₂ capture *Energy Procedia*. 2009;1:1083-1089.
 - [3] McCann N., Maeder M., Attalla M.. Simulation of enthalpy and capacity of CO₂ absorption by aqueous amine systems *Ind. Eng. Chem. Res.*. 2008;47:2002-2009.
 - [4] Feron P. H. M.. Exploring the potential for improvement of the energy performance of coal fired power plants with post-combustion capture of carbon dioxide *Int. J. GHG Control*. 2010;4:152-160.
 - [5] Oyenekan B. A., Rochelle G. T.. Alternative stripper configurations for CO₂ capture by aqueous amines *AIChE Journal*. 2007;53:3144-3154.
 - [6] Oexmann J., Kather A.. Minimising the regeneration heat duty of post-combustion CO₂ capture by wet chemical absorption: The misguided focus on low heat of absorption solvents *Int. J. GHG Control*. 2010;4:36-43.
 - [7] House K. Z., Harvey C. F., Aziz M. J., Schrag D. P.. The energy penalty of post-combustion CO₂ capture & storage and its implications for retrofitting the US installed base *Energy Environ. Sci.*. 2009;2:193-205.
 - [8] Leites I. L., Sama D. A., Lior N.. The theory and practice of energy saving in the chemical industry: some methods for reducing thermodynamic irreversibility in chemical technology processes *Energy*. 2003;28:55-97.
 - [9] Gabrielsen J., Michelsen M. L., Stenby E. H., Kontogeorgis G. M.. A model for estimating CO₂ solubility in aqueous alkanolamines *Ind. Eng. Chem. Res.*. 2005;44:3348-3354.
 - [10] Gabrielsen J.. *CO₂ capture from coal fired power plants*. PhD thesis Technical University of Denmark 2007.
 - [11] Mathias P. M., Reddy S., O'Connell J. P.. Quantitative evaluation of the chilled-ammonia process for CO₂ capture using thermodynamic analysis and process simulation *Int. J. GHG Control*. 2010;4:174-179.
 - [12] Oyenekan B. A., Rochelle G. T.. Energy performance of stripper configurations for CO₂ capture by aqueous amines *Ind. Eng. Chem. Res.*. 2006;45:2457-2464.
 - [13] Weiland R. H., Dingman J. C., Cronin D. Benjamin. Heat capacity of aqueous monoethanolamine, diethanolamine, *N*-methyl-diethanolamine, and *N*-methyl-diethanolamine-based blends with carbon dioxide *J. Chem. Eng. Data*. 1997;42:1004-1006.